START- ON-THE- PART TRANSIENT MODEL FOR *IN-SITU* AUTOMATED TAPE PLACEMENT OF THERMOPLASTIC COMPOSITES

Robert C. Costen
NASA Langley Research Center
Hampton, VA

Joseph M. Marchello
Old Dominion University
Norfolk, VA

ABSTRACT

Fabrication of a complex part by automated tape placement (ATP) can require starting up a new tape-end in the part interior, termed "start-on-the-part." Careful thermal management of the starting transient is needed to achieve uniform crystallinity and inter-laminar weld strength -- which is the objective of this modeling effort. The transient is modeled by a Fourier-Laplace transform solution of the time-dependent thermal transport equation in two spatial dimensions. The solution is subject to a quasi-steady approximation for the speed and length of the consolidation head. Sample calculations are done for the Langley ATP robot applying PEEK/carbon fiber composite and for two upgrades in robot performance. The head starts out almost at rest – which meets an engineering requirement for accurate placement of the new tape-end. The head then rapidly accelerates until it reaches its steady state speed. This rapid acceleration, however, violates the quasi-steady approximation, so uniform weld strength and crystallinity during the starting transient are not actually achieved. The solution does give the elapsed time and distance from start-up to validity of the quasi-steady approximation -- which quantifies the length of the non-uniform region. The elapsed time was always less than 0.1 s and the elapsed distance less than 1 cm. This quantification would allow the non-uniform region to be either trimmed away or compensated for in the design of a part. Such compensation would require experiments to measure the degree of non-uniformity, because the solution does not provide this information. The rapid acceleration suggests that the consolidation roller or belt be actively synchronized to avoid abrading the tape.

KEY WORDS: Modeling, Carbon Fibers, Thermoplastic Polymers, Composites, PEEK/C.

---

1. INTRODUCTION

In the *in situ* automated tape placement (ATP) process, carbon fiber/thermoplastic composite tape is spooled out and progressively welded under heat and pressure to a previous layer in order to build up a laminated composite panel. Often the tape is laid from edge to edge on the supporting tool to create a uniform panel. Then the tape ends are trimmed away to eliminate the effects of the starting and stopping transients. The corresponding steady state ATP process has been modeled extensively, as, for example, in refs. 1-6.

Some applications, however, require the panel to have non-uniform thickness. Such can be fabricated by starting a new tape-end at an interior point of the panel instead of at its edge. This advanced procedure is called "start-on-the-part." It causes an initial thermal transient that can alter the inter-laminar weld strength and crystalline state near the new tape-end. Also, the initial speed must be reduced to place the new tape-end accurately. The objective of this research is to maintain uniform strength and crystallinity during start-on-the-part while allowing for reduced initial speed.

The modeling approach is to find a quasi-steady solution of the time-dependent thermal transport equation and determine the effects of the thermal transient on the effective bonding time, t_{eff}, and the final crystalline state. (According to reptation theory, the inter-laminar weld strength after wetting occurs is proportional to $t_{eff}^{1/4}$ until full strength is reached (ref. 2).) The speed U and length x_h of the consolidation head are then varied with time to achieve a uniform t_{eff} and crystalline state.

2. TIME-DEPENDENT MODEL

The start-on-the-part configuration being modeled is shown in Fig. 1, except that the consolidation head actually conforms around the new tape end to make continuous contact. The model uses a two-dimensional approximation that is valid when the Peclet number $\mathrm{Pe} >> 1$, where Pe is the dimensionless ratio of inertial to diffusive heat transport (ref. 3). The origin of the (x,y) coordinate system is located at the nip, where the time-dependent thermal input $q(t)$ (in W m^{-1}) is applied. For $t < 0, q = 0$, and for $t \geq 0, q = q_0 = \text{const}$. The thermal conductivities of the supporting tool and the consolidation head are taken to be the same as the average thermal conductivity of the laminated composite substrate. At distances far away from the nip, the temperatures in the tool and in the head are maintained at T_∞ (usually room temperature). Subject to these idealizations, the thermal transport equation is given by

$$\rho C_p \frac{\partial T}{\partial t} + \rho C_p U \frac{\partial T}{\partial x} = K_{11} \frac{\partial^2 T}{\partial x^2} + K_{22} \frac{\partial^2 T}{\partial y^2} + q_0 \delta(x)\delta(y)H(t) \qquad (1)$$

where $T(x,y,t)$ is the temperature, ρ is the density, C_p is the specific heat at constant pressure, K_{11} and K_{22} are the tensor thermal conductivity components, $\delta(x)$ and $\delta(y)$ are Dirac delta functions, and $H(t)$ is the unit step function.

The thermal input q_0 is constrained so that in the steady state $(t = \infty)$ the temperature on the weld interface $(y = 0)$ decreases passively to the glass transition temperature T_g at the downstream end of the consolidation head x_h. This constraint is given by

$$T\left[x_h(\infty),0,\infty\right]=T_g \tag{2}$$

As mentioned, U and x_h are both functions of t. Dimensionless (primed) quantities can be defined as follows:

$$T'\equiv\frac{T-T_\infty}{T_g-T_\infty} \tag{3a}$$

$$q_0'\equiv\frac{q_0}{2\pi\left(K_{11}K_{22}\right)^{1/2}\left(T_g-T_\infty\right)} \tag{3b}$$

$$b\equiv\frac{\rho C_p U(t)x_h(t)}{2K_{11}}=\frac{\mathrm{Pe}}{2} \tag{3c}$$

$$x'\equiv\frac{x}{x_h(t)} \tag{3d}$$

$$y'\equiv\left(\frac{K_{11}}{K_{22}}\right)^{1/2}\frac{y}{x_h(t)} \tag{3e}$$

$$t'\equiv\frac{U(t)}{x_h(t)}t \tag{3f}$$

The partial derivatives then become

$$\frac{\partial}{\partial x}=\frac{1}{x_h}\frac{\partial}{\partial x'} \tag{3g}$$

$$\frac{\partial}{\partial y}=\frac{1}{x_h}\left(\frac{K_{11}}{K_{22}}\right)^{1/2}\frac{\partial}{\partial y'} \tag{3h}$$

$$\frac{\partial}{\partial t}=\left[t\frac{\partial}{\partial t}\left(\frac{U}{x_h}\right)+\frac{U}{x_h}\right]\frac{\partial}{\partial t'}\approx\frac{U}{x_h}\frac{\partial}{\partial t'} \tag{3i}$$

As indicated by the preceding equation, the quasi-steady approximation requires that

$$\frac{t\,x_h}{U}\frac{\partial}{\partial t}\left(\frac{U}{x_h}\right)<<1 \tag{4}$$

Then (1) becomes

$$2b\frac{\partial T'}{\partial t'}+2b\frac{\partial T'}{\partial x'}=\frac{\partial^2 T'}{\partial x'^2}+\frac{\partial^2 T'}{\partial y'^2}+2\pi q_0'\delta(x')\delta(y')H(t') \tag{5}$$

This equation is solvable analytically if b is a constant; i.e., $U(t')x_h(t')=\text{const}$. Taking the partial t'- derivative gives

$$2b\frac{\partial\tau'}{\partial t'}+2b\frac{\partial\tau'}{\partial x'}=\frac{\partial^2\tau'}{\partial x'^2}+\frac{\partial^2\tau'}{\partial y'^2}+2\pi q_0'\delta(x')\delta(y')\delta(t') \tag{6}$$

where $\tau'\equiv\partial T'/\partial t'$. Equation (6) can now be solved by the method of Fourier and Laplace transforms to give

$$\tau'(x',y',t')=\frac{q_0'}{2t'}\exp\left[-\frac{b}{2}\left(\frac{x'^2+y'^2}{t'}+t'-2x'\right)\right] \tag{7}$$

and

$$T'(x',y',t')=\frac{q_0'}{2}\int_0^{t'}\frac{1}{t*}\exp\left[-\frac{b}{2}\left(\frac{x'^2+y'^2}{t*}+t*-2x'\right)\right]dt* \tag{8}$$

where $t*$ is a dummy variable of integration. The constraint (2) is given in dimensionless variables by

$$T'(1,0,\infty)=1 \tag{9}$$

Its application to (8) yields

$$q_0'=\frac{1}{\exp(b)K_0(b)} \tag{10}$$

where K_0 is a hyperbolic Bessel function. In the quasi-steady approximation, this equation is assumed to hold during the transient. It provides a physical means for maintaining a constant b by maintaining a constant thermal input. Substituting (10) into (8) gives finally the constrained temperature

$$T'(x',y',t')=\frac{1}{2\exp(b)K_0(b)}\int_0^{t'}\frac{1}{t*}\exp\left[-\frac{b}{2}\left(\frac{x'^2+y'^2}{t*}+t*-2x'\right)\right]dt* \tag{11}$$

3. THERMAL TRANSIENT

Equation (11) can be used to plot the isotherms of dimensionless temperature for various values of b and t'. The nature of the thermal transient in the composite substrate during start-on-the-part is shown in Fig. 2 for $b=100$. (The transient in the head is a mirror image.) For small values of t' (Fig. 2(a)), the welding heat is confined to a small region near the nip. As t' increases (Fig. 2(b)), the heat penetrates more deeply into the substrate and is transported farther downstream. Finally, the steady state is reached (Fig. 2(c)) when the $T'=1$ isotherm intersects the x'-axis at $x'=1$, in accordance with the constraint (9). (The isotherms shown in Fig. 2 are exact when U and x_h are both held constant at their steady values during the transient. For variable U and x_h such that $Ux_h=$ const., the validity of the isotherms depends on the validity of the quasi-steady approximation.)

4. QUASI-STEADY APPROXIMATION (CONTINUED)

The condition for the validity of the quasi-steady approximation is given by (4). Besides (10), another steady state relationship is assumed to hold during the transient. This relationship, as presented in ref. 5, is

$$\Delta t(T') = \frac{\pi}{4}\left(\frac{K_{22}}{K_{11}}\right)^{1/2} \frac{{x_h}^2}{Ud}\Delta x'_+(T')y'_{\max}(T') \tag{12}$$

Here, $\Delta x'_+(T')$ is the positive segment of the x'-axis that is enclosed by the T'-isotherm, $y'_{\max}(T')$ is the maximum penetration of the T'-isotherm into the substrate, d is the thickness of the tape, and $\Delta t(T')$ is the total period that the dimensionless temperature of a material point on the weld interface equals or exceeds T'. The period $\Delta t(T')$ includes the initial heating and subsequent reheating as more plies are added. Only the positive segment of the x'-axis is included because only the combination of heat and pressure contributes to welding.

5. UNIFORM INTER-LAMINAR WELD STRENGTH

For ideal welding, the maximum temperature approaches but remains slightly less than the degradation temperature T_d. Under these conditions, ref. 5 shows that t_{eff} is directly proportional to $\Delta t(T_d')$, where T_d' is the dimensionless degradation temperature. Therefore, uniform inter-laminar weld strength requires that $\Delta t(T_d') = \text{const.}$ during the starting transient. A more general condition is that $\Delta t(T_p') = \text{const.}$; i.e.

$$\frac{x_h(t')^2}{U(t')}\Delta x'_+(T_p',t')y'_{\max}(T_p',t') = \frac{x_h(\infty)^2}{U(\infty)}\Delta x'_+(T_p',\infty)y'_{\max}(T_p',\infty) \tag{13}$$

where T_p' is a parametric temperature. For uniform weld strength, $T_p' = T_d'$. Since $b = \text{const.}, U(t') \propto x_h(t')^{-1}$ and (13) can be solved for $U(t')$

$$U(t') = \alpha(t')^{1/3}U(\infty) \tag{14a}$$

or for $x_h(t')$

$$x_h(t') = \alpha(t')^{-1/3}x_h(\infty) \tag{14b}$$

where

$$\alpha(t') \equiv \frac{\Delta x'_+(T_p',t')y'_{\max}(T_p',t')}{\Delta x'_+(T_p',\infty)y'_{\max}(T_p',\infty)} \tag{14c}$$

The time t is related to dimensionless time t' by (3f)

$$t = t'\frac{x_h(t')}{U(t')} = t'\alpha(t')^{-2/3}\frac{x_h(\infty)}{U(\infty)} \tag{14d}$$

Finally, (11) can be used to determine $y'_{\max}(T_p',t')$ and $\Delta x'_+(T_p',t')$, which are then substituted in (14c) to give $\alpha(t')$, as follows: For any t', the value of y' as a function of x' is given implicitly for the T_p'-isotherm by the equation

$$\int_0^{t'} \frac{1}{t^*} \exp\left[-\frac{b}{2}\left(\frac{x'^2 + y'^2}{t^*} + t^* - 2x' \right) \right] dt^* - 2T_p' \exp(b) K_0(b) = 0 \qquad (14e)$$

The maximum penetration of the T_p'-isotherm occurs at the point on the isotherm where $\partial y'/\partial x' = 0$. Taking the partial x'-derivative of (14e) with T_p' held fixed and setting $\partial y'/\partial x' = 0$ gives

$$\int_0^{t'} \frac{1}{t^*}\left(1 - \frac{x'}{t^*}\right) \exp\left[-\frac{b}{2}\left(\frac{x'^2 + y'^2}{t^*} + t^* - 2x' \right) \right] dt^* = 0$$

(14f)

Solving (14e) and (14f) simultaneously for a given t' gives $y'_{\max}(T_p', t')$ and the corresponding value of x'. (This value of x' is discarded since it is not needed.)

For a given t', the value $\Delta x'_+(T_p', t')$ is obtained by setting $y' = 0$ in (11)

$$\int_0^{t'} \frac{1}{t^*} \exp\left[-\frac{b}{2}\left(\frac{x'^2}{t^*} + t^* - 2x' \right) \right] dt^* - 2T_p' \exp(b) K_0(b) = 0 \qquad (14g)$$

and solving for the positive x'-root.

Figure 2 shows that as t' increases, the high temperature isotherms are the first to achieve their steady shapes. Therefore, the starting transient is very brief for achieving uniform inter-laminar weld strength, which is based on the highest parametric temperature $T_p' = T_d'$.

6. UNIFORM CRYSTALLINE STATE

According to ref. 6, the final crystalline state is determined by the cooling rates through the crystallization zone T_{c1} to T_{c0}, where $T_{c0} < T_{c1}$. Achieving a uniform crystalline state during start-up requires that $\Delta t(T_{c0}') = \text{const.}$ All of the formulas of section 5 then apply with $T_p' = T_{c0}'$. Since it takes longer for the T_{c0}'-isotherm to reach its steady shape, the starting transient will last longer and uniform weld strength will also be achieved. A more conservative requirement is that $\Delta t(T_g') = \text{const.}$, which is implemented by setting $T_p' = T_g' = 1$.

7. EXAMPLES

Sample start-on-the-part calculations of $U(t)$ and $x_h(t)$ are done for the Langley ATP robot applying PEEK/carbon fiber composite. Present operating conditions of the robot correspond to $b \approx 10$. Calculations are also done for two upgrades in robot performance, which correspond to $b = 100$ and $b = 1000$. These upgrades result from proportional increases in the steady state head speed $U(\infty)$ and consolidation length $x_h(\infty)$. Increases in $x_h(\infty)$ are a natural consequence of making the head more conformable.

The relevant material parameters are $\rho = 1560\ \text{kg m}^{-3}$, $C_p = 1425\ \text{J kg}^{-1}\ \text{K}^{-1}$, $K_{11} = 6\ \text{W m}^{-1}\ \text{K}^{-1}$, $K_{22} = 0.72\ \text{W m}^{-1}\ \text{K}^{-1}$, $T_d = 823\ \text{K}$, $T_{c0} = 453\ \text{K}$, and $T_g = 413\ \text{K}$. The corresponding values for the parametric temperature T_p' are $T_d' = 4.42$, $T_{c0}' = 1.33$, and

$T_g' = 1$. The fixed process parameters are $T_\infty = 293\,\mathrm{K}$, $d = 1.27\times10^{-4}\,\mathrm{m}$, and tape width $w = 3.175\times10^{-2}\,\mathrm{m}$.

For the first calculation $(b = 10)$, the input power $Q_0 = wq_0 = 127\,\mathrm{W}$, and the steady speed and length of the consolidation head are given by $U(\infty) = 0.0425\,\mathrm{m\,s^{-1}}$ and $x_h(\infty) = 1.27\times10^{-3}\,\mathrm{m}$. Plots of U and x_h versus t are shown in Fig. 3 for the three values of T_p' discussed. Also plotted is the elapsed distance of the head from its starting point $S(t) \equiv \int_0^t U(t^*)dt^*$. Each of the plots is divided in two by a vertical line. The quasi-steady approximation (4) is valid to the right of the vertical line and invalid to the left.

In the second calculation $(b = 100)$, $Q_0 = 397\,\mathrm{W}$, $U(\infty) = 0.134\,\mathrm{m\,s^{-1}}$, and $x_h(\infty) = 4.02\times10^{-3}\,\mathrm{m}$ and the results are plotted in Fig. 4. The third calculation $(b = 1000)$ has $Q_0 = 1{,}255\,\mathrm{W}$, $U(\infty) = 0.425\,\mathrm{m\,s^{-1}}$, and $x_h(\infty) = 0.0127\,\mathrm{m}$ and the results are plotted in Fig. 5. The elapsed times and distances from the initiation of start-up until the quasi-steady approximation becomes valid are summarized in Tables 1 and 2.

Table 1. Elapsed time t (in s) from start-up to validity of the quasi-steady approx.

b	$T_p' = T_d' = 4.42$	$T_p' = T_{c0}' = 1.33$	$T_p' = T_g' = 1$
10	.0217	.058	.080
100	.0058	.030	.058
1000	.0042	.030	.042

Table 2. Elapsed distance S (in m) from start-up to validity of the quasi-steady approx.

b	$T_p' = T_d' = 4.42$	$T_p' = T_{c0}' = 1.33$	$T_p' = T_g' = 1$
10	.0007	.0018	.0024
100	.0006	.0025	.0052
1000	.0013	.0083	.0098

8. DISCUSSION

At first glance, the plots seem disappointing because the underlying quasi-steady approximation is seen to be invalid for nearly all of the transient period. Hence, the goal of uniform weld strength and crystallinity during the starting transient was not achieved. The reason is that the transients are very steep. This steepness is advantageous, however, because it implies that the regions of non-uniformity are small. As shown in Table 2, the non-uniform regions are shorter than 1 cm for the sample calculations and sometimes much shorter. This table quantifies how much of the new tape end needs to be machined away to achieve uniformity or, alternatively, how large a non-uniform area needs to be compensated for when designing a laminate. Since the model does not quantify the degree of non-uniformity, experiments are needed that measure the variations in strength and crystallinity in the non-uniform region.

Figures 3 to 5 show that the head starts moving slowly and then accelerates rapidly to its steady speed. This slow start is exactly what is needed for accurate placement of the new tape end. The rapid acceleration of the head is necessary if the region of non-uniformity is to be kept short. Such acceleration makes it advisable to actively synchronize the consolidation

roller or belt so that the tape is not abraded. These figures also show that the consolidation head is initially long and rapidly shrinks to its steady length. In concept, a trailing shoe could be lowered to exert extended pressure during the starting transient and then raised upon reaching the steady state. However, Table 1 shows that the duration of the starting transient is less that 0.1 s for the sample calculations. This short time period appears to make the concept of a retractable shoe impractical.

9. CONCLUSIONS

The modeling objectives for start-on-the-part have been partially achieved. The time-dependent thermal transport equation was solved subject to a quasi-steady approximation that was intended to give uniform weld strength and crystallinity during the starting transient. The resulting solution shows that the head is initially almost at rest -- in agreement with the engineering requirement for accurate placement of the new tape-end. The head then rapidly accelerates until it reaches its steady speed.

This rapid acceleration, however, violates the quasi-steady approximation, so uniform weld strength and crystallinity during the starting transient are not actually achieved. The solution does give the elapsed time and distance from start-up to validity of the quasi-steady approximation -- which quantifies the length of the non-uniform region. This quantification would allow the non-uniform region to be either trimmed away or compensated for in the design of a panel. Such compensation would require experiments to measure the degree of departure from uniformity, since the solution does not provide this information. The rapid acceleration suggests that the consolidation roller or belt be actively synchronized to avoid abrading the tape.

REFERENCES

1. S. Mantell, Q. Wang, and G. S. Springer, *SAMPE International Symposium, 36*, 1763-1772 (1996).
2. J. A. Hinkley, J. M. Marchello , and B. C. Messier, NASA TM-110203 (1996).
3. R. Pitchumani, R. C. Don, J. W. Gillespie, Jr., and S. Ranganathan in V. Prasad *et al.*, eds., *HTD-Vol. 289, Thermal Processing of Materials: Thermal Mechanics, Controls and Composites*, ASME, 223-234 (1994).
4. R. G. Irwin, Jr. and S. I. Güçeri, *AMD-Vol. 194, Mechanics in Materials Processing and Manufacturing*, ASME, 319-333 (1994).
5. R. C. Costen and J. M. Marchello, *SAMPE International Symposium, 42*, 33-47 (1997).
6. F. O. Sonmez and H. T. Hahn, *J. Thermoplastic Composite Materials, 10*, 198-240 (1997).

BIOGRAPHIES

Robert C. Costen is an applied mathematician at NASA-Langley who works in the Composites and Polymers Branch. He has authored and co-authored numerous modeling papers in materials processing, aerodynamics, atmospheric science, lasers, and radiation protection.

Joseph M. Marchello is a professor of civil and mechanical engineering at Old Dominion University. He is a chemical engineer with over 30 years of teaching and research experience in process development. He is author of over 100 technical and scientific papers.

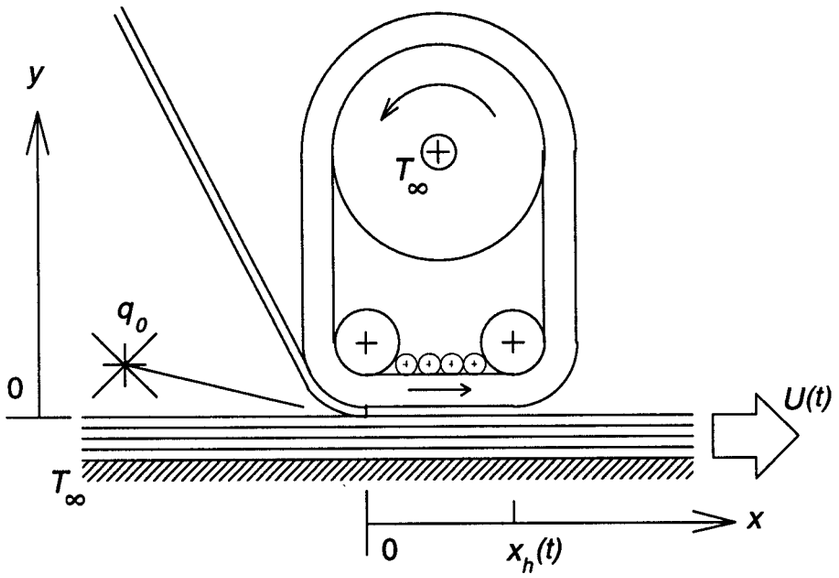

Figure 1. Start-on-the-part configuration at $t = 0$. The consolidation head actually conforms around the new tape-end to make continuous contact from $x = 0$ to $x = x_h$.

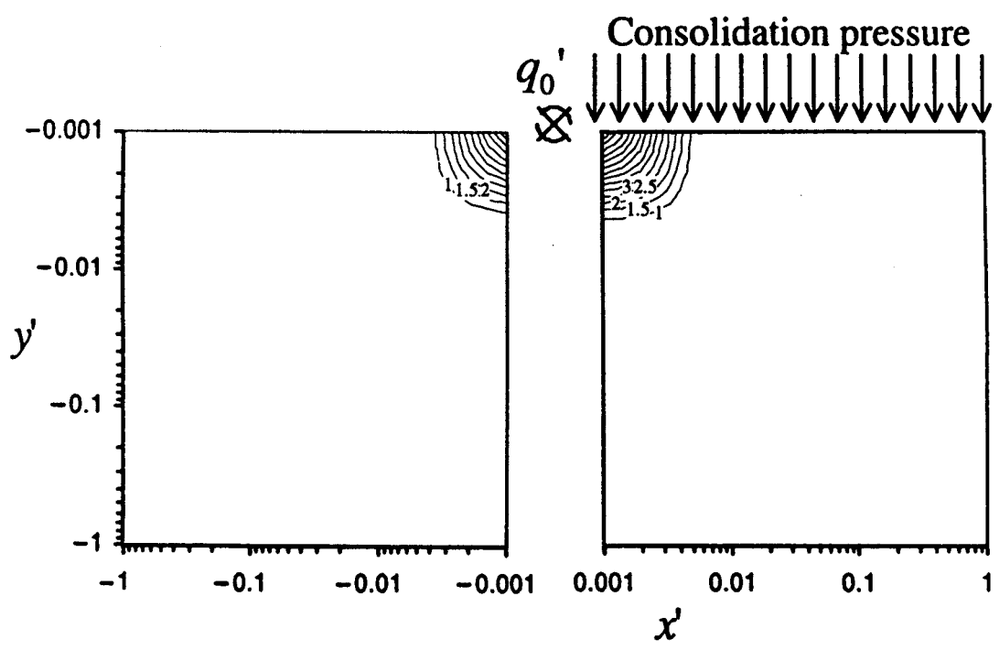

(a) $t' = 0.001$

Figure 2. Isotherms of dimensionless temperature T' in composite substrate for $b = Pe/2 = 100$ and various dimensionless times t' during start-on-the-part.

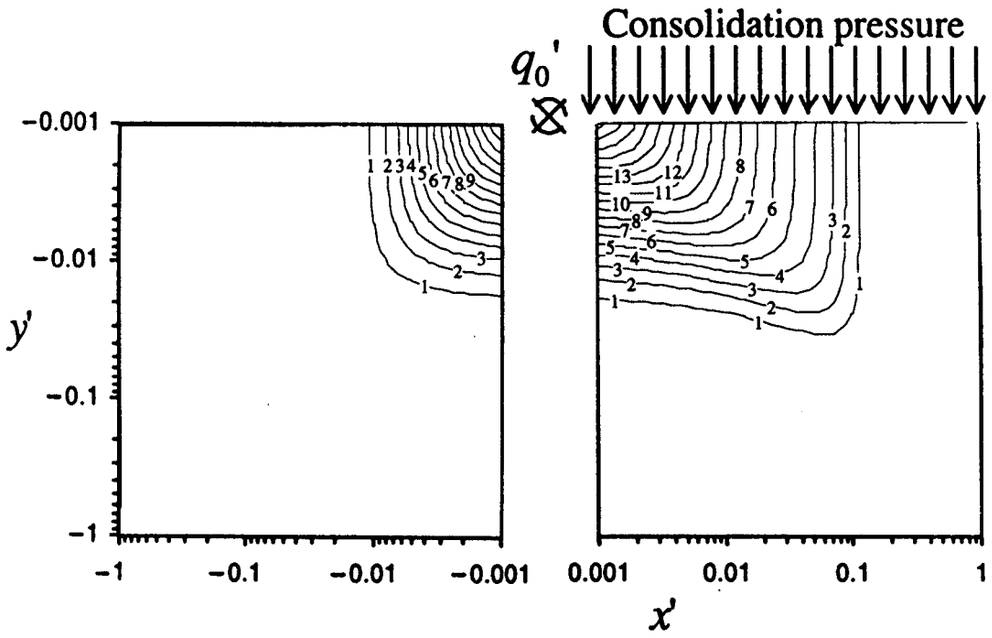

(b) $t' = 0.1$

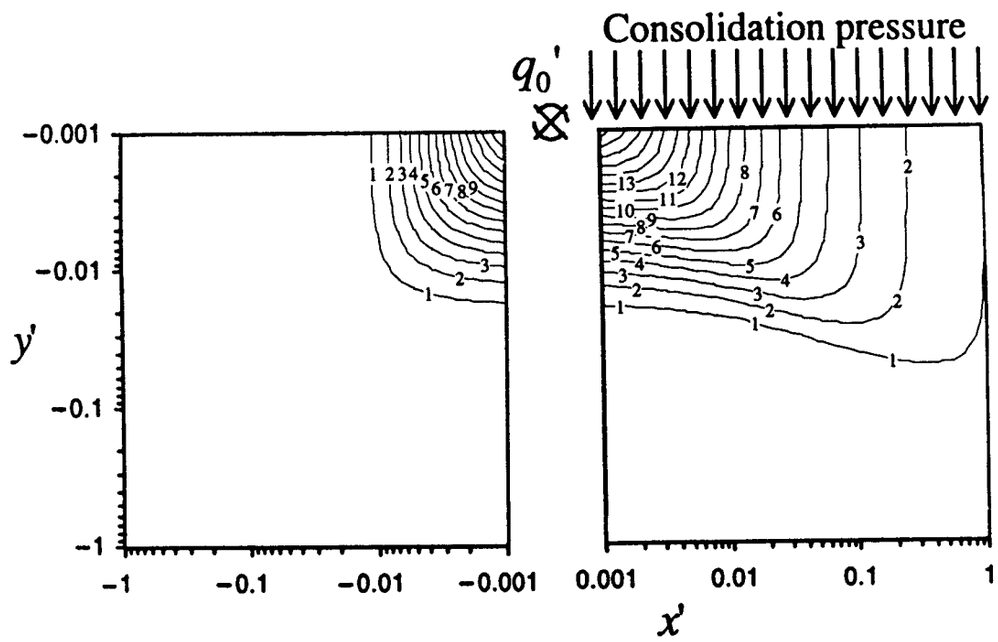

(c) $t' = 10$

Figure 2. Concluded.

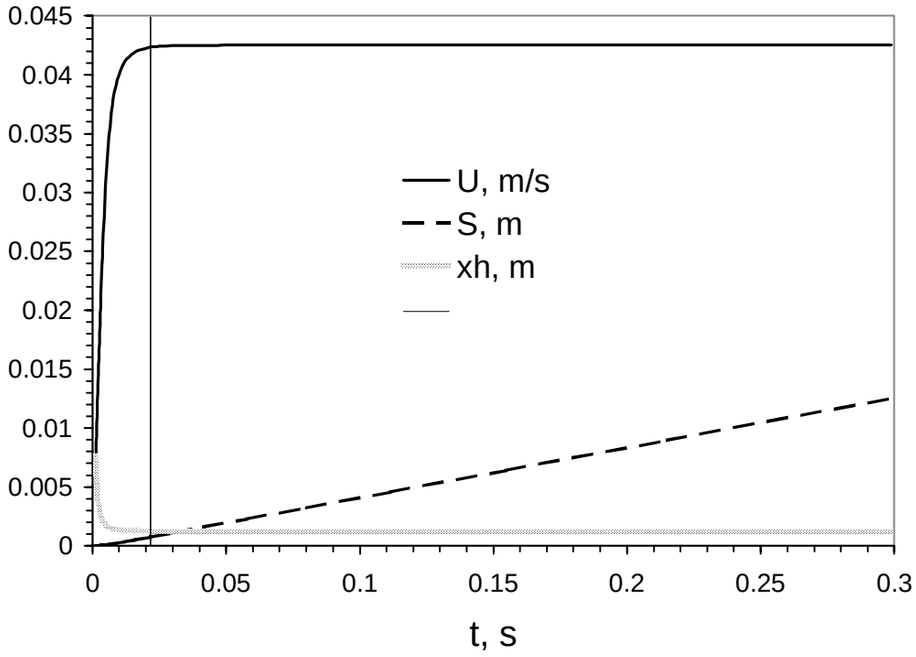

(a) $T_p' = T_d' = 4.42$

Figure 3. Model head speed U, elapsed distance S, and consolidation length x_h versus time t for $b = Pe/2 = 10$ and various dimensionless parametric temperatures T_p'.

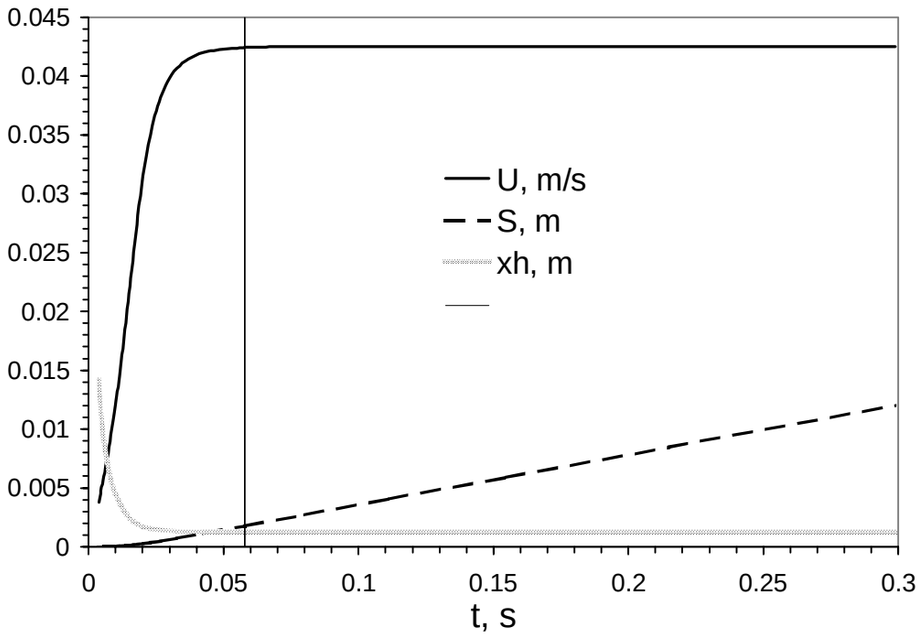

(b) $T_p' = T'_{c0} = 1.33$

Figure 3. Continued.

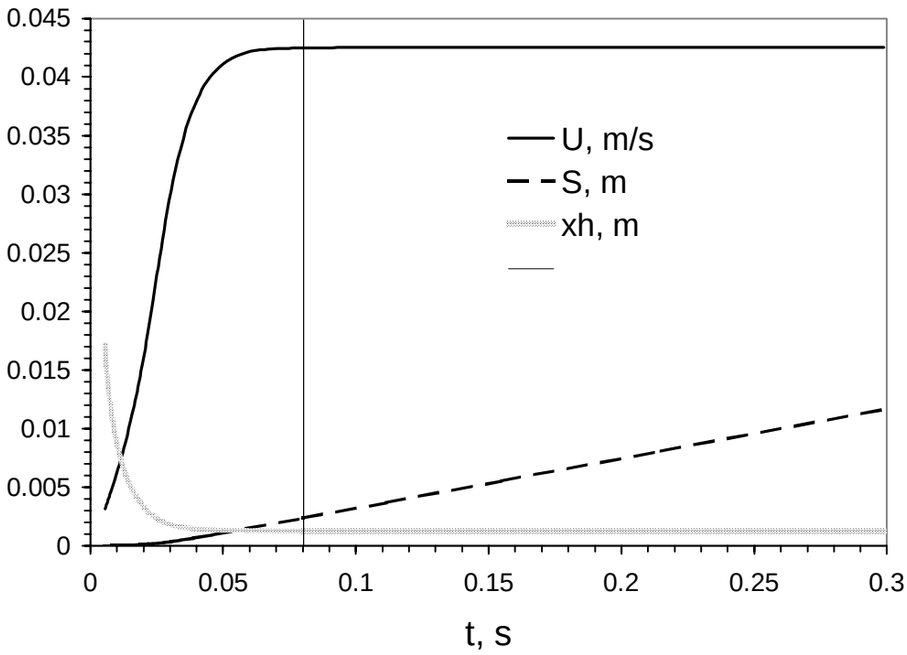

(c) $T_p' = T_g' = 1$

Figure 3. Concluded.

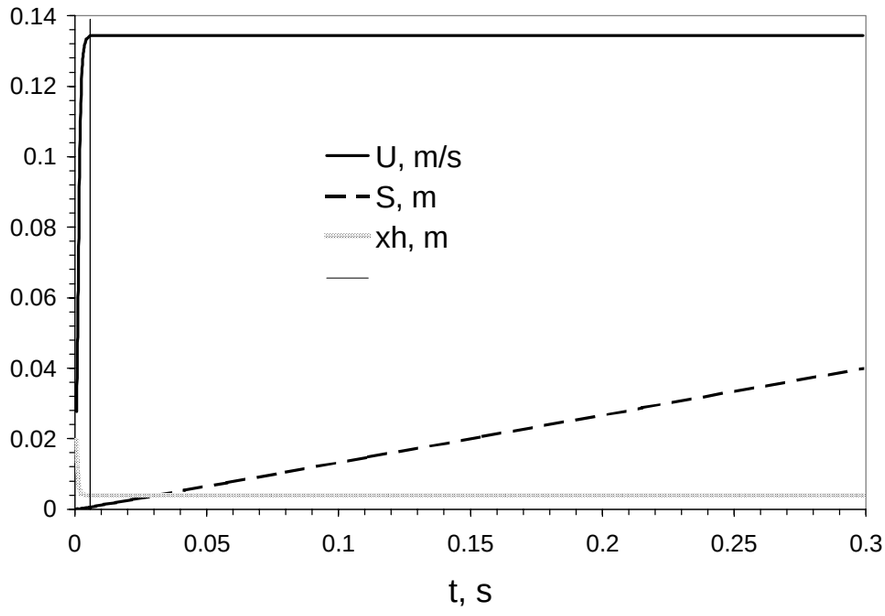

(a) $T_p' = T_d' = 4.42$

Figure 4. Model head speed U, elapsed distance S, and consolidation length x_h versus time t for $b = Pe/2 = 100$ and various dimensionless parametric temperatures T_p'.

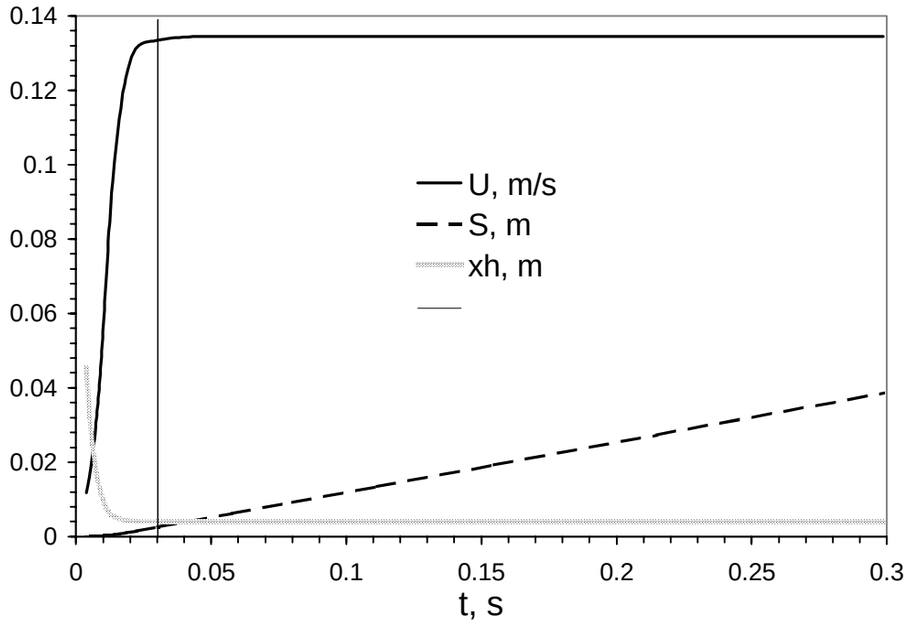

(b) $T_p' = T'_{c0} = 1.33$

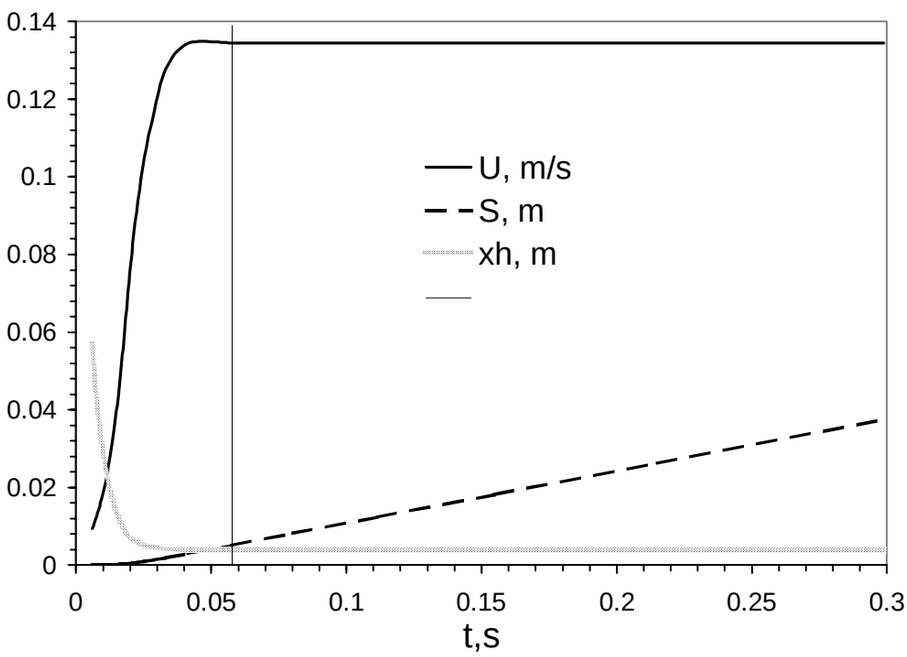

(c) $T_p' = T_g' = 1$

Figure 4. Concluded.

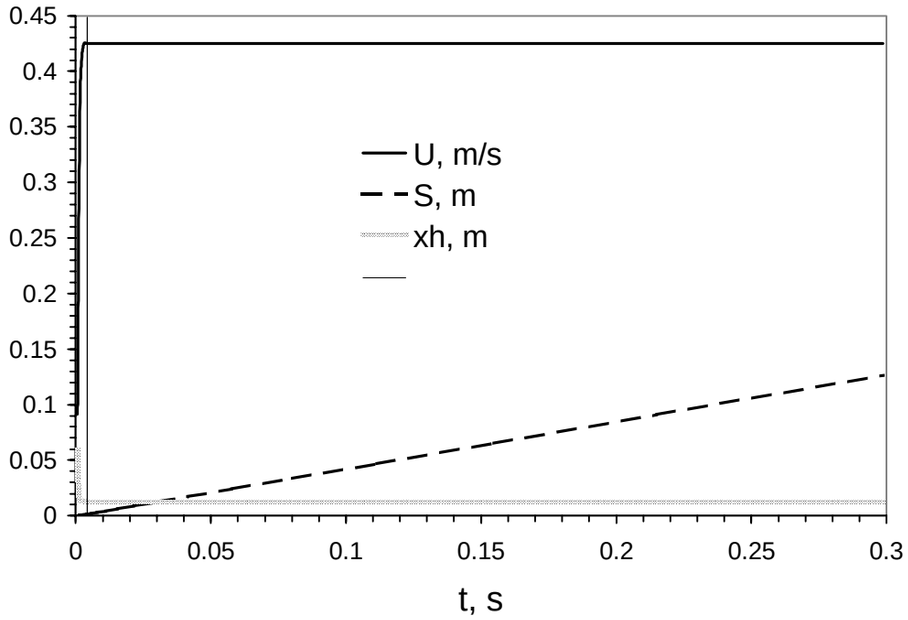

(a) $T_p' = T_d' = 4.42$

Figure 5. Model head speed U, elapsed distance S, and consolidation length x_h versus time t for $b = Pe/2 = 1000$ and various dimensionless parametric temperatures T_p'.

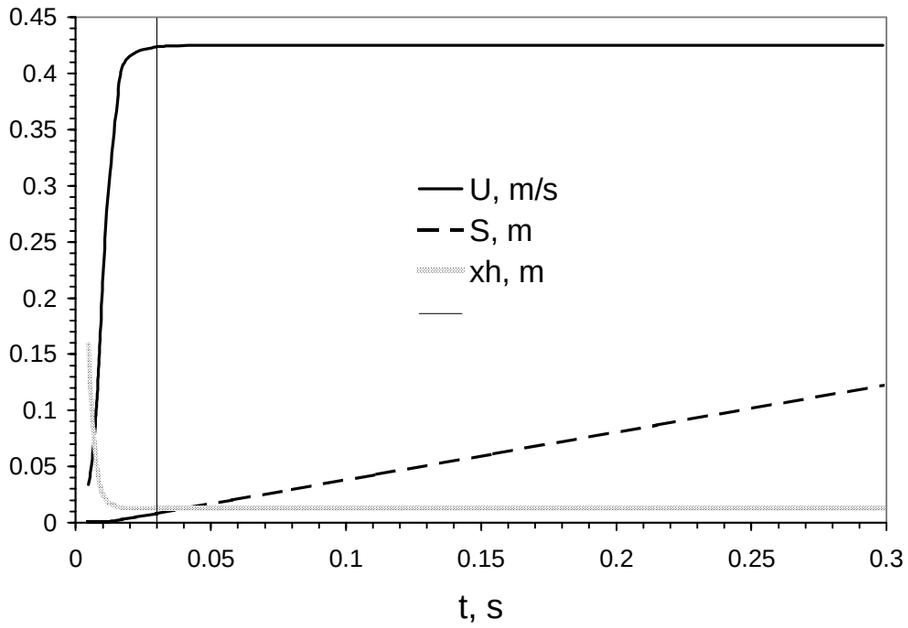

(b) $T_p' = T'_{c0} = 1.33$

Figure 5. Continued.

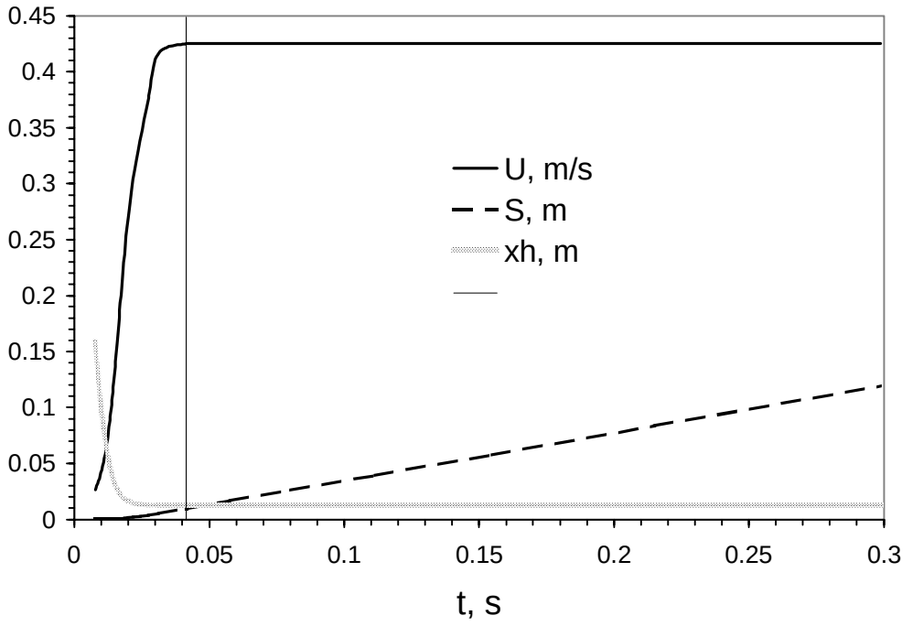

(c) $T_p' = T_g' = 1$

Figure 5. Concluded.